



Published in final edited form as:

Cell Rep. 2021 October 26; 37(4): 109904. doi:10.1016/j.celrep.2021.109904.

## Peli1 facilitates NLRP3 inflammasome activation by mediating ASC ubiquitination

Lingyun Zhang<sup>1,3,8</sup>, Chun-Jung Ko<sup>1,8</sup>, Yanchuan Li<sup>1</sup>, Zuliang Jie<sup>1,4</sup>, Lele Zhu<sup>1</sup>, Xiaofei Zhou<sup>1</sup>, Xiaoping Xie<sup>1,5</sup>, Tianxiao Gao<sup>1,6</sup>, Ting Liu<sup>1,7</sup>, Xuhong Cheng<sup>1</sup>, Shao-Cong Sun<sup>1,2,9,\*</sup>

<sup>1</sup>Department of Immunology, The University of Texas MD Anderson Cancer Center, 7455 Fannin Street, Box 902, Houston, TX, USA

<sup>2</sup>MD Anderson Cancer Center UT Health Graduate School of Biomedical Sciences, Houston, TX, USA

<sup>3</sup>Present address: Center for Reproductive Medicine, Henan Key Laboratory of Reproduction and Genetics, The First Affiliated Hospital of Zhengzhou University, Zhengzhou, China

<sup>4</sup>Present address: State Key Laboratory of Cellular Stress Biology, Innovation Center for Cell Biology, School of Life Sciences, Xiamen University, Xiamen, China

<sup>5</sup>Present address: AbbVie, 1000 Gateway Boulevard, South San Francisco, CA 94080, USA

<sup>6</sup>Present address: Sun Yat-sen University Cancer Center, State Key Laboratory of Oncology in South China, Collaborative Innovation Center for Cancer Medicine, Guangzhou, China

<sup>7</sup>Present address: Department of Laboratory Medicine, West China Second University Hospital, State Key Laboratory of Biotherapy and Collaborative Innovation Center for Biotherapy, Sichuan University, Chengdu, China

<sup>8</sup>These authors contributed equally

<sup>9</sup>Lead contact

### SUMMARY

Inflammasomes are crucial for innate immunity against infections and, when deregulated, also contribute to inflammatory diseases. Here, we identify a critical function of the E3 ubiquitin ligase Peli1 in regulating the activation of NLRP3 inflammasome. Peli1 deficiency impairs induction of interleukin-1 $\beta$  (IL-1 $\beta$ ) secretion by different NLRP3 inducers, but not by inducers of

This is an open access article under the CC BY-NC-ND license (<http://creativecommons.org/licenses/by-nc-nd/4.0/>).

\*Correspondence: ssun@mdanderson.org.

#### AUTHOR CONTRIBUTIONS

Lingyun Zhang and Chun-Jung Ko designed and performed research, analyzed data, and prepared the figures; Chun-Jung Ko wrote the manuscript; Yanchuan Li, Zuliang Jie, Lele Zhu, Xiaofei Zhou, Xiaoping Xie, and Tianxiao Gao assisted with animal experiments, sample processing, and/or data analysis; Ting Liu performed experiments; Xuhong Cheng assisted with animal experiments; and Shao-Cong Sun supervised the work and wrote the manuscript.

#### SUPPLEMENTAL INFORMATION

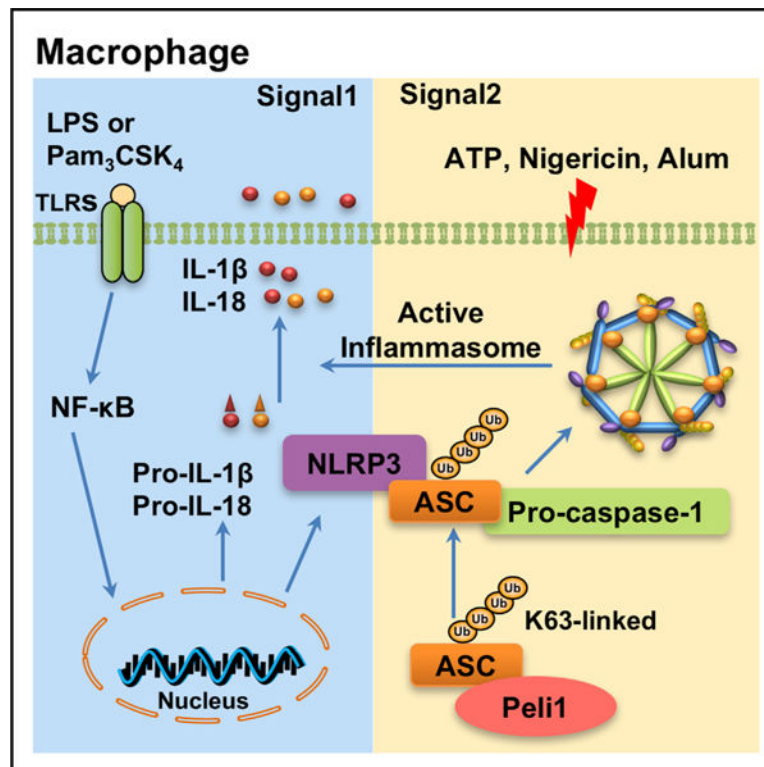
Supplemental information can be found online at <https://doi.org/10.1016/j.celrep.2021.109904>.

#### DECLARATION OF INTERESTS

X.X. is presently an employee of AbbVie, a company headquartered in Lake County, IL, although his contribution to this work was made while he was employed at the University of Texas MD Anderson Cancer Center. The remaining authors declare no competing interests.

the Aim2, NLRP1, and NLRC4 inflammasomes. Peli1-deficient mice have alleviated peritonitis induction by alum and display increased resistance to lipopolysaccharide (LPS) endotoxin shock, coupled with decreased serum concentration of IL-1 $\beta$ . Peli1 is required for NLRP3-induced caspase-1 activation and IL-1 $\beta$  maturation. Mechanistically, Peli1 conjugates K63 ubiquitin chain to lysine 55 of the inflammasome adaptor apoptosis-associated speck-like protein containing a caspase recruitment domain (ASC), which in turn facilitates ASC/NLRP3 interaction and ASC oligomerization, thereby contributing to inflammasome activation. Peli1 deficiency impairs the ubiquitination of ASC and inhibits inflammasome activation. Our findings establish Peli1 as an important inflammasome regulator and suggest a mechanism by which Peli1 mediates inflammatory responses.

## Graphical abstract



## In brief

Inflammasome activation is crucial for host defense against infections and also contributes to inflammatory disorders, but the mechanism regulating inflammatory activation is incompletely understood. Zhang et al. demonstrate that the E3 ubiquitin ligase Peli1 is important for NLRP3 inflammasome activation and inflammasome-associated inflammatory responses in mice.

## INTRODUCTION

Inflammasomes are multiprotein intracellular complexes that detect pathogenic microorganisms and environmental stress and mediate activation of inflammatory caspases

required for the processing and secretion of proinflammatory cytokines, including interleukin-1 $\beta$  (IL-1 $\beta$ ) and IL-18 (Broz and Dixit, 2016). While inflammasomes are critical components of innate immunity against infections, deregulated inflammasome activation is associated with various diseases, including autoimmunity, inflammatory disorders, and neurodegenerative diseases (Guo et al., 2015). Targeting inflammasome pathways provides an important approach for developing therapeutic approaches to treat inflammatory diseases (Zahid et al., 2019).

Several types of inflammasomes have been characterized, including NLRP3, NLRP1, NLRC4, and AIM2 inflammasomes, among which the NLRP3 inflammasome is the best studied (Yang et al., 2019). The NLRP3 inflammasome complex is composed of the ligand-sensing receptor NLRP3, the adaptor protein ASC, pro-caspase-1, and the regulatory protein NIMA-related kinase 7 (NEK7) (Broz and Dixit, 2016) (Swanson et al., 2019). In response to diverse stimuli, NLRP3 undergoes oligomerization and recruits pro-caspase-1 via the adaptor ASC, and the oligomer formation triggers the conversion of pro-caspase-1 into active caspase-1, which in turn cleaves pro-IL-1 $\beta$  and pro-IL-18, leading to secretion of these proinflammatory cytokines (Swanson et al., 2019). NLRP3 inflammasome activation also requires a priming signal, which is typically mediated by pattern-recognition receptors (PRRs) as a response to microbial components. A primary role of the priming signal is to induce the expression of NLRP3 (Swanson et al., 2019). Emerging evidence suggests that inflammasome activation is subject to tight regulation, although the underlying mechanisms are incompletely understood.

Protein ubiquitination plays an important role in regulating PRR signaling and innate immune and inflammatory responses (Hu and Sun, 2016). In particular, the Pellino family of E3 ubiquitin ligases have been implicated in the regulation of Toll-like receptor (TLR) signaling and inflammation (Jin et al., 2012; Moynagh, 2014). We have previously shown that Peli1 conjugates lysine 63 (K63)-linked polyubiquitin chains to the signaling adaptor RIP1, thereby mediating activation of nuclear factor  $\kappa$ B (NF- $\kappa$ B) signaling and induction of proinflammatory cytokine gene expression (Chang et al., 2009). This function of Peli1 is specific for TIR-domain-containing adapter-inducing interferon- $\beta$  (TRIF)-dependent TLRs, while Peli1 is dispensable for NF- $\kappa$ B activation by the MyD88-dependent TLRs and IL-1 receptor (IL-1R). In the present study, we demonstrate that Peli1 has a crucial role in NLRP3 inflammasome activation. Peli1-deficient macrophages have attenuated secretion of IL-1 $\beta$  and IL-18 when primed by both TRIF-dependent and MyD88-dependent TLRs and stimulated by different NLRP3 inducers. Consistently, Peli1-knockout (Peli1-KO) mice are refractory to peritonitis induction by the NLRP3 inducer alum. We further show that Peli1 promotes ASC speck formation and oligomerization by mediating K63-linked ubiquitination of ASC. Our data establish Peli1 as an important regulator of NLRP3 inflammasome activation and provide insight into the mechanism by which Peli1 participates in inflammatory responses.

## RESULTS

### Peli1 deficiency alleviates alum-induced peritonitis

To investigate the function of Peli1 in regulating inflammation, we employed a model of peritonitis induced by the NLRP3 inflammasome inducer alum, a widely used adjuvant that not only enhances antigen uptake by dendritic cells but also promotes leukocyte recruitment via induction of NLRP3-inflammasome-dependent IL-1 $\beta$  secretion (Eisenbarth et al., 2008; Sokolovska et al., 2007). As previously reported (Guarda et al., 2011), alum induced a drastic increase in the number of peritoneal exudate cells (PECs) (Figure 1A). Importantly, the alum-induced PEC increase was severely attenuated in Peli1-KO mice (Figure 1A). Analysis of the PEC populations revealed that alum treatment increased the numbers of Ly6G<sup>hi</sup> neutrophils and Ly6C<sup>hi</sup> inflammatory monocytes in wild-type (WT) mice; however, the induction of both cell populations was attenuated in Peli1-KO mice (Figure 1A). Since alum-induced peritonitis involves induction of IL-1 $\beta$  secretion, we measured the concentration of IL-1 $\beta$  in the peritoneal lavage fluid by ELISA. In line with these results, Peli1-KO mice also had significantly reduced levels of IL-1 $\beta$  in peritoneal lavage (Figure 1B).

To determine the proinflammatory function of Peli1 in innate immune cells, we performed alum-induced peritonitis using Peli1 myeloid-cell-conditional-KO (MKO; *Peli1*<sup>fl/fl</sup>Ly2-Cre) or WT control (*Peli1*<sup>+/+</sup>Ly2-Cre) mice. As seen with germline Peli1-KO mice (Figures 1A and 1B), Peli1-MKO mice were largely defective in alum-induced increase in PECs, including both neutrophils and monocytes, as well as in the induction of IL-1 $\beta$  (Figures 1C and 1D). This result was not due to differences in myeloid cell development or homeostasis, since WT and Peli1-MKO mice had comparable frequencies of peripheral blood macrophages, neutrophils, and monocytes under homeostatic conditions (Figure S1). To further determine the role of Peli1 in regulating IL-1 $\beta$ -associated inflammation, we employed a model of LPS-induced shock, which is known to be dependent on IL-1 $\beta$  and IL-18 (Vanden Berghe et al., 2014). Compared with WT control mice, Peli1-MKO mice were significantly more resistant to LPS-induced lethality and showed significantly reduced serum concentrations of IL-1 $\beta$ , but not tumor necrosis factor  $\alpha$  (TNF- $\alpha$ ) or IL-6 (Figure 1E and 1F). Together, these results demonstrate an important role for Peli1 in mediating alum- and LPS-induced acute inflammation and indicate the involvement of Peli1 in inflammasome activation in myeloid cells.

### Peli1 facilitates NLRP3 inflammasome activation in macrophages

To directly determine the function of Peli1 in regulating inflammasome activation, we examined the effect of Peli1 deficiency on inflammasome-mediated secretion of IL-1 $\beta$  and IL-18. To this end, we employed a widely used two-signal model of inflammasome activation in bone-marrow-derived macrophages (BMDMs), involving priming cells with LPS followed by stimulation with activators of the NLRP3 inflammasome (ATP, nigericin, and alum), AIM2 inflammasome (poly(dA:dT)), NLRC4 inflammasome (Flagellin), and NLRP1 inflammasome (muramyl dipeptide [MDP]) (He et al., 2016; Schroder and Tschoopp, 2010). Compared to WT BMDMs, Peli1-deficient BMDMs secreted a profoundly lower level of IL-1 $\beta$  and IL-18 in response to the NLRP3 inducers ATP, nigericin, and alum

(Figure 2A). The overall level of IL-1 $\beta$ /IL-18 induction by the other inflammasome sensors was low and was only moderately reduced in Peli1-deficient BMDMs (Figures 2A and S2A). Peli1 deficiency also attenuated LPS-stimulated production of TNF- $\alpha$  and IL-6, but this result was independent of the inflammasome inducers (Figure S2B), which was in line with our previous finding that Peli1 facilitates TRIF-dependent signaling (Chang et al., 2009). These results suggested that in addition to regulating TRIF-dependent signaling, Peli1 might play a role in NLRP3 inflammasome activation. To further evaluate this possibility, we examined NLRP3 inflammasome activation based on procaspase-1 activation and pro-IL-1 $\beta$  maturation. Peli1 deficiency impaired generation and secretion of the mature IL-1 $\beta$  p17 and active caspase-1 p20 (Figure 2B). Notably, Peli1-deficient BMDMs did not show an obvious defect in the expression of NLRP3 or pro-IL-1 $\beta$ , suggesting that Peli1 might play a role in mediating NLRP3 inflammasome activation instead of priming. Since inflammasome activation is associated with pyroptosis (Xue et al., 2019), we assessed the role of Peli1 in regulating pyroptosis induction based on the release of a cytoplasmic enzyme, lactate dehydrogenase (LDH) (Rayamajhi et al., 2013). Indeed, Peli1 deficiency significantly reduced the release of LDH in macrophages stimulated by LPS plus nigericin (Figure S2C).

We have previously shown that Peli1 is involved in NF- $\kappa$ B activation by TRIF-dependent TLRs, but not MyD88-dependent TLRs (Chang et al., 2009). To further examine the role of Peli1 in mediating NLRP3 activation, we primed the BMDMs with Pam<sub>3</sub>CSK<sub>4</sub>, an agonist of the MyD88-dependent TLR2. Similar to the results of LPS priming, Peli1 deficiency significantly reduced the level of IL-1 $\beta$  secretion in response to the NLRP3 activators ATP and nigericin (Figure 2C). On the other hand, the Peli1 deficiency did not influence TNF- $\alpha$  induction (Figure 2C). Immunoblotting analysis confirmed the role of Peli1 in mediating NLRP3 inflammasome activation, as evidenced by the impaired generation of mature IL-1 $\beta$  p17 and activated caspase-1 p20 in Peli1-deficient BMDMs (Figure 2D). Since alum and poly(dA:dT) did not induce caspase-1 processing or IL-1 $\beta$  maturation, we repeated the experiment by increasing the treatment time of alum and poly(dA:dT). Under these conditions, both alum and poly(dA:dT) stimulated caspase-1 processing and IL-1 $\beta$  maturation (Figure S2D). Importantly, Peli1 deficiency substantially impaired the caspase-1 processing and IL-1 $\beta$  maturation induced by the NLRP3 inducer alum and moderately inhibited these molecular events induced by the AIM2 inducer poly(dA:dT) (Figure S2D).

LPS-induced lethality is known to involve a non-canonical inflammasome pathway relying on activation of caspase-11 (Kayagaki et al., 2011). We thus also examined the effect of Peli1 on non-canonical inflammasome activation induced by transfected LPS. In contrast to the canonical NLRP3 inflammasome activation, the non-canonical inflammasome activation was not affected by Peli1 deficiency, as suggested by the comparable caspase-11 cleavage and IL-1 $\beta$  secretion (Figures S3A and S3B). LPS transfection stimulated the production of TNF- $\alpha$  and IL-6, which was partially inhibited in Peli1-KO BMDMs (Figure S3B). This latter result was probably due to TLR4 stimulation by extracellular LPS. These results suggest that Peli1 is involved in the activation of canonical, but not non-canonical, NLRP3 inflammasomes.

To further assess the involvement of NLRP3 inflammasome in Peli1-mediated regulation of inflammatory responses, we employed a selective inhibitor of the NLRP3 inflammasome, MCC950 (Coll et al., 2015). MCC950 dramatically suppressed the induction of IL-1 $\beta$  secretion by the NLRP3 inducer nigericin in WT BMDMs (Figure S3C). On the other hand, MCC950 only moderately inhibited IL-1 $\beta$  induction in Peli1-deficient BMDMs, consistent with the already attenuated NLRP3 activation in these mutant macrophages (Figure S3C). Furthermore, MCC950 efficiently protected WT mice from endotoxin-induced lethality, largely erasing the differences between WT and Peli1 KO mice (Figure 2E). Consistently, MCC950 treatment also reduced the serum concentration of IL-1 $\beta$  in WT mice to a level similar to that of the Peli1 KO mice (Figure 2F). Taken together, these data suggest that Peli1 has a crucial role in mediating canonical NLRP3 inflammasome activation and NLRP3-dependent inflammation.

### **Peli1 regulates the formation of ASC speck upon NLRP3 inflammasome activation**

Activation of NLRP3 inflammasome involves aggregation of the adaptor ASC and formation of microscopically visible specks (Broz et al., 2010; Fernandes-Alnemri et al., 2007; Lu et al., 2014). Immunofluorescence staining of ASC detected specks in BMDMs primed with LPS and activated by nigericin (Figures 3A and 3B). Importantly, Peli1 deficiency significantly reduced the frequency of cells with ASC specks (Figures 3A and 3B). Formation of ASC dimers and oligomers was also profoundly attenuated in Peli1-deficient BMDMs compared with WT BMDM (Figure 3C). Similarly, Peli1 deficiency also attenuated the formation of ASC dimers and oligomers in BMDMs primed with LPS or Pam3CSK4 and activated by ATP (Figure 3D).

To examine whether overexpressed Peli1 promotes ASC speck formation, we employed a NLRP3 inflammasome reconstitution model (Shi et al., 2016). In brief, we transfected HEK293 cells with expression vectors for NLRP3, NEK7, caspase-1, and ASC with or without Peli1 (Figure S4A). Under such overexpression conditions, a low number of cells with ASC specks was detected under untreated conditions, and ASC speck formation was increased upon stimulation of the cells with the NLRP3 inducer nigericin (Figures S4B and S4C). Importantly, Peli1 expression significantly promoted the ASC speck formation under both untreated and nigericin-stimulated conditions (Figures S4B and S4C). These data indicate that Peli1 facilitates NLRP3 inflammasome activation by regulating ASC oligomerization and speck formation.

### **Peli1 mediates ASC ubiquitination**

Since Peli1 is an E3 ubiquitin ligase, we examined whether it was involved in the ubiquitination of any component of the NLRP3 inflammasome. In response to stimulation by LPS or LPS plus nigericin, NLRP3 was conjugated with polyubiquitin chains; however, the NLRP3 ubiquitination was not appreciably affected by the Peli1 deficiency (Figure S5A). The NLRP3 inflammasome activation was also associated with ASC ubiquitination, which was particularly strong when the cells were stimulated with LPS together with the NLRP3 inducer nigericin (Figure 4A). The inducible ASC ubiquitination was attenuated in Peli1-deficient primary BMDMs (Figure 4A). To assure that this result was not due to developmental effect, we performed small hairpin RNA (shRNA)-mediated Peli1



knockdown using immortalized BMDMs (Figure S5B). Silencing Peli1 using two different shRNAs led to potent inhibition of ASC ubiquitination (Figure 4B). These results suggest that Peli1 is required for induction of endogenous ASC ubiquitination along with NLRP3 activation. Parallel experiments revealed that the ASC ubiquitination was strongly induced by several NLRP3 inducers but only weakly induced by the other inflammasome inducers (Figure 4C).

To examine whether Peli1 was sufficient for inducing ASC ubiquitination, we transfected HEK293T cells with ASC in the absence or presence of Peli1. Expression of WT Peli1 potently induced ASC ubiquitination (Figure 4D). This function of Peli1 was dependent on its catalytic activity, since a Peli1 mutant lacking the C-terminal RING domain (Peli1<sup>C</sup>) failed to ubiquitinate ASC (Figure 4D). Because Peli1 is capable of catalyzing both K48 and K63 ubiquitination chains (Jin et al., 2012; Moynagh, 2009), we further analyzed Peli1-mediated ASC ubiquitination using ubiquitin mutants harboring lysine-to-arginine mutations in all lysine residues except lysine 48 (ubiquitin K48) or lysine 63 (ubiquitin K63). Peli1 efficiently catalyzed the conjugation of WT ubiquitin and ubiquitin K63 to ASC but only weakly conjugated ubiquitin K48 to ASC (Figure 4E). Consistently, mutation of lysine 63 (K63R), but not lysine 48 (K48R), of ubiquitin abolished its conjugation to ASC by Peli1 (Figure 4F). These results suggest that Peli1 predominantly conjugates K63-linked polyubiquitin chains to ASC.

To further delineate the mechanism by which Peli1 mediated ubiquitination, we tested whether Peli1 might physically interact with ASC. Coimmunoprecipitation (CoIP) assays revealed a weak interaction between Peli1 and ASC in untreated BMDMs; this interaction was strongly induced by LPS, although it was not further enhanced by nigericin (Figure 4G). Peli1 also interacted with ASC when coexpressed in HEK293T cells (Figure 4H). A Peli1 mutant lacking the C-terminal RING domain (Peli1<sup>C</sup>) retained the ASC-binding ability, whereas a Peli1 mutant lacking the N-terminal domain (Peli1<sup>N</sup>) lost the ASC-binding function (Figure 4H), suggesting that the N-terminal domain of Peli1 is required for interaction with ASC. These findings suggest that Peli1 physically interacts with, and catalyzes K63 ubiquitination of, ASC.

### **Peli1-mediated ASC ubiquitination is required for NLRP3 inflammasome activation**

To define the site of Peli1-induced ASC ubiquitination, we generated human ASC mutants harboring lysine-to-arginine substitutions at different lysine residues (Figures 5A and 5B). Mutation of K55 reduced Peli1-mediated ASC ubiquitination, whereas mutation of the other lysine residues did not appreciably interfere with ASC ubiquitination (Figure 5C). By using the ubiquitin K63 mutant, we further showed that K55 of ASC was critical for its K63 ubiquitination by Peli1 (Figure 5D). Notably, K55 of ASC is highly conserved across the species (Figure 5E). We further analyzed whether K55 of murine ASC was also required for its ubiquitination conjugation by Peli1. As seen with human ASC, mutation of K55 in murine ASC markedly reduced Peli1-induced ASC ubiquitination (Figure 5F). These results thus identified K55 of ASC as a critical residue for its ubiquitin conjugation induced by Peli1.

To assess the functional significance of ASC ubiquitination in NLRP3 activation, we silenced ASC expression by shRNA in immortalized BMDMs (iBMDMs). As expected, ASC knockdown in iBMDMs inhibited LPS/nigericin-stimulated IL-1 $\beta$  maturation and secretion (Figure 6A). We then reconstituted the ASC-knockdown iBMDMs with WT ASC or K55 mutant. Stimulation of the reconstituted cells with LPS and nigericin triggered poly-ubiquitination of WT ASC, but not ASC K55R mutant (Figure 6B). Furthermore, WT ASC, but not ASC K55 mutant, rescued the ASC-knockdown iBMDMs in LPS/nigericin-stimulated generation and secretion of active caspase-1 (p20) and mature IL-1 $\beta$  (p17) (Figure 6C). The impaired function of K55R in supporting LPS/nigericin-induced IL-1 $\beta$  secretion was also confirmed by ELISA (Figure 6D). Furthermore, the ASC K55R mutant displayed impaired function in mediating induction of IL-1 $\beta$  secretion by different NLRP3 inducers (Figure S6). The K55R mutation of ASC also moderately affected IL-1 $\beta$  induction by the AIM2, NLRC4, and NLRP1 inflammasome activators; however, these results did not reach statistical significance (Figure S6).

ASC has an N-terminal pyrin domain (PYD) that mediates interaction with the PYD of NLRP3 as well as ASC self-association, which are crucial for NLRP3 inflammasome assembly and activation (Vajjhala et al., 2012). Since the ubiquitination site of ASC (K55) is located in the PYD, we examined whether ASC ubiquitination might play a role in facilitating the interaction between ASC and NLRP3 and ASC oligomerization. We performed coIP assays using the ASC-knockdown iBMDMs reconstituted with WT or K55R mutant form of ASC. LPS/nigericin treatment induced the binding of NLRP3 with ASC in cells reconstituted with WT ASC, but this inducible NLRP3/ASC binding was attenuated in cells reconstituted with the K55R ASC mutant (Figure 6E). In further support a role for Peli1-induced ASC ubiquitination in facilitating the ASC/NLRP3 interaction, Peli1 overexpression in HEK293 cells could also induce the binding of NLRP3 to WT ASC, but not ASC K55R mutant (Figure 6F). Moreover, the K55R mutation of ASC also profoundly attenuated LPS/nigericin-induced ASC oligomerization (Figure 6G). These findings suggest that Peli1-mediated ASC ubiquitination facilitates the interaction of ASC with NLRP3 and ASC oligomerization, which may contribute to the mechanism by which Peli1 regulates NLRP3 inflammasome activation.

## DISCUSSION

The results presented in this paper demonstrated a ubiquitin-dependent mechanism regulating NLRP3 inflammasome activation. This mechanism requires the E3 ubiquitin ligase Peli1, which conjugates K63-linked ubiquitin chains to the adaptor protein ASC, which in turn is crucial for NLRP3 inflammasome activation. Peli1 deficiency impaired the induction of IL-1 $\beta$  secretion by different NLRP3 inducers and alleviates alum-induced peritonitis in mice. These results demonstrate a novel mechanism by which Peli1 regulates inflammation and emphasizes the role of ASC ubiquitination in the regulation of NLRP3 ubiquitination.

We have previously shown that Peli1 facilitates NF- $\kappa$ B activation by TRIF-dependent, but not MyD88-dependent, TLRs in embryonic fibroblasts and BMDMs (Chang et al., 2009). Peli1 deficiency impairs poly(IC)- and LPS-induced expression of a subset of



proinflammatory cytokine genes, including *Tnf*, *Il6*, and *Il12b*. Peli1 mediates K63 ubiquitination of RIP1, a signaling adaptor involved in TRIF-dependent TLR signaling (Chang et al., 2009). Our present study demonstrated a critical role for Peli1 in mediating NLRP3 inflammasome activation. Peli1 deficiency impaired the induction of caspase-1 activation and pro-IL-1 $\beta$  processing by NLRP3 inducers. Although NF- $\kappa$ B is involved in induction of NLRP3 expression, our data suggest that Peli1 deficiency did not substantially reduce the induction of NLRP3 protein expression in LPS-primed macrophages. Thus, it is unlikely that the impaired NLRP3 inflammasome activation in Peli1-KO was due to a defect in the priming. This conclusion is further supported by our finding that Peli1 deficiency also impaired NLRP3 inflammasome activation primed by Pam3Csk4, an agonist of the MyD88-dependent TLR2.

In line with the *in vitro* studies using BMDMs, mice with myeloid-cell-specific Peli1 deficiency (*Peli1* MKO) were substantially more protective against alum-induced peritonitis and LPS-induced lethality, associated with reduced IL-1 $\beta$  production. We have previously shown that Peli1 deficiency also attenuates lethality induced by LPS plus D-galactosamine (Chang et al., 2009), an acute inflammation model that is largely dependent on TNF- $\alpha$  (Pasparakis et al., 1996; Pfeffer et al., 1993). Of note, in contrast to the LPS/D-galactosamine model (Chang et al., 2009), the LPS lethality model did not show a significant difference in TNF- $\alpha$  production between WT and Peli1-deficient mice. This discrepancy may be attributed to the different conditions used. First, the LPS/D-galactosamine model used whole-body *Peli1*-KO mice, whereas the LPS lethality model used *Peli1*-MKO mice. Second, since D-galactosamine (a liver-specific transcription inhibitor) enhances the toxicity of LPS, the LPS/D-galactosamine model uses a substantially lower dose of LPS (0.1  $\mu$ g/mouse or  $\sim$ 4  $\mu$ g/kg body weight) than the LPS model (25 mg/kg body weight). Notwithstanding, our present study demonstrated that an NLRP3 inhibitor efficiently protects WT mice from LPS-induced lethality and largely erases the differences between WT and Peli1-KO mice, emphasizing the *in vivo* role of Peli1 in NLRP3 inflammasome regulation.

We obtained biochemical and genetic evidence suggesting the direct involvement of Peli1 in NLRP3 inflammasome activation. We found that Peli1 physically interacts with ASC and is required for signal-induced ASC oligomerization and speck formation. ASC undergoes ubiquitination along with NLRP3 activation, which is impaired in Peli1-deficient macrophages. Transfection studies further demonstrated that Peli1 conjugates K63 ubiquitin chains to ASC. A highly conserved ubiquitination site of ASC, K55, is located in its PYD and required for the function of ASC in mediating NLRP3 inflammasome activation. Since the PYD of ASC mediates interaction with the PYD of NLRP3 as well as ASC self-association (Vajjhala et al., 2012), it is likely that PYD ubiquitination may facilitate the PYD/PYD interaction. In support of this idea, we found that Peli1 induces the ASC/NLRP3 interaction in a K55-dependent manner. K55R mutation of ASC also impairs its oligomerization induced by NLRP3 inducers. A prior study suggests that in response to RNA viral infections, the mitochondrial adaptor protein MAVS recruits the E3 ubiquitin ligase TRAF3 to ASC for K63 ubiquitination of ASC at K174, which is critical for ASC speck formation and optimal inflammasome activation (Guan et al., 2015). The Peli1 homolog Peli2 also plays a role in NLRP3 inflammasome activation (Humphries et al., 2018). Unlike Peli1, Peli2 mediates NLRP3 ubiquitination during LPS-induced priming.

These findings, along with our present observations, highlight a ubiquitin-dependent mechanism that modulates inflammasome activation by viruses and classical NLRP3 activators. The results reported in the present study also suggest that Peli1 participates in inflammatory responses via different mechanisms.

The dynein adaptor histone deacetylase 6 (HDAC6) displays functional selectivity in mediating inflammasome activation; it is required for activation of NLRP3 and pyrin inflammasomes, but not NLRP4, AIM2, and non-canonical inflammasomes (Magupalli et al., 2020). HDAC6 appears to act by binding to ubiquitinated NLRP3 complex, likely via ubiquitinated ASC (not NLRP3), and dynein, thereby transporting the NLRP3 inflammasome to the microtubule-organizing center (MTOC) for activation (Magupalli et al., 2020). Although NLRP4 and AIM2 also associate with ASC, they are not located at the MTOC and do not depend on HDAC6 for activation, although the underlying mechanism remains unclear. Notably, our present study revealed that Peli1 also displays functional selectivity in inflammasome activation; it is required for activation of the NLRP3 inflammasome, but not NLRP1, NLRP4, AIM2, or non-canonical inflammasomes. Our data suggest that the activators of NLRP3, but not NLRP1, NLRP4, and AIM2, induced ASC ubiquitination, together with LPS. Future studies will examine whether Peli1 is required for MTOC transportation of the NLRP3 inflammasome.

## STAR★METHODS

### RESOURCE AVAILABILITY

**Lead contact**—Further information, and request for resources and reagents should be directed to the lead contact, Dr. Shao-Cong Sun (ssun@mdanderson.org).

**Materials availability**—Any new generated materials from this study can be shared upon request to the Lead contact and with an approved MTA.

#### Data and code availability

- All data reported in this paper will be shared by the lead contact upon request.
- This paper does not report original code.
- Any additional information required to reanalyze the data reported in this paper is available from the lead contact upon request.

### EXPERIMENTAL MODEL AND SUBJECT DETAILS

**Mouse models**—Peli1-flox mice were generated as described (Ko et al., 2021). Briefly, the Peli1-targeted mice, Peli1<sup>tm1a(EUCOMM)Wtsi</sup> (in C57BL/6N genetic background), were created from ES cell clone Peli1\_B06 generated by the European Conditional Mouse Mutagenesis Program and made into mice by the KOMP Repository (<https://www.komp.org/>) and the Mouse Biology Program (<https://mbp.mousebiology.org/>) at the University of California Davis. Methods used to create EUCOMM targeted alleles were as described (Testa et al., 2004). Live mice were generated in the Genetically Engineered Mouse Facility of MD Anderson Cancer Center using the sperms obtained from KOMP.

The *Peli1*-targeted mice were crossed with FLP delete mice (Rosa26-FLPe; C57BL/6J background; Jackson Laboratory) to produce *Peli1*-flox mice, which were further crossed with *Lyz2*-Cre mice (Jackson Laboratory) to generate conditional KO mice with *Peli1* specifically deleted in myeloid cells (*Peli1<sup>fl/fl</sup>**Lyz2*-Cre; MKO) and WT control mice (*Peli1<sup>+/+</sup>**Lyz2*-Cre). Germline *Peli1* KO mice were generated as previously described (Chang et al., 2009). Heterozygous mice were bred to generate KO and WT littermates. 6–8 week-old and sex-matched (male and female) KO and WT mice were used for experiments. Mice were maintained in a specific pathogen-free facility, and all animal experiments were in accordance with protocols approved by the Institutional Animal Care and Use Committee of the University of Texas MD Anderson Cancer Center.

**Cell cultures**—Human embryonic kidney cell line 293T was originally obtained from the American Type Culture Collection (ATCC). Murine immortalized bone marrow-derived macrophage (iBMDM) was obtained from BEI Resources. The cell lines were cultured in DMEM supplemented with 10% FBS, 2 mM L-glutamine, 1% sodium pyruvate, and 1% penicillin-streptomycin in a humidified, 5% CO<sub>2</sub> incubator at 37°C.

## METHOD DETAILS

**Plasmid generation**—Expression vectors encoding Myc-epitope tagged ASC mutants with K to R substitutions, K21,22,24,26R, K55R, K109R, K139R, K158,161R, and K274R, were generated by site-directed mutagenesis (QuickChange II Site-Directed Mutagenesis Kit, Agilent) using pcDNA3-Myc-ASC as template. pcDNA3-Flag-ASC K55R and pCI-ASC-HA K55R were generated by site-directed mutagenesis using pcDNA3-Flag-ASC and pCI-ASC-HA, respectively, as template. Myc-ASC and Myc-ASC K55 were subcloned into the pMSCV-IRES-mCherry retroviral vector. The primers used for cloning and site-directed mutagenesis were listed in Table S1.

**Alum-Induced Peritonitis**—8-week-old of WT and *Peli1* KO Mice were injected intraperitoneally with 1 mg alum dissolved in 0.2ml warm sterile PBS. 14 hours later, Mice were euthanized by CO<sub>2</sub> overdose, and infiltrating cells were harvested by peritoneal lavage with 5 mL PBS, counted and stained with cell surface markers. For IL-1 $\beta$  secretion studies, Mice were also euthanized 6 hours after injection of alum and peritoneal cavities were flushed with 5 mL ice-cold PBS, and then the fluid was clarified by centrifugation and IL-1 $\beta$  was analyzed by ELISA after concentration using an Amicon Ultra 10K filter from Millipore.

**Inflammasome activation assay**—Cells were primed with LPS (1  $\mu$ g/ml) or Pam<sub>3</sub>CSK<sub>4</sub> (500 ng/ml) for 3.5 h followed by stimulation with the inflammasome activators in serum-free DMEM medium: Nigericin (5  $\mu$ M), adenosine 5' -triphosphate disodium salt hydrate (ATP) (5 mM) for additional 30 mins, or alum (300  $\mu$ g/ml), Poly (dA:dT) (5  $\mu$ g/ml), Flagellin (1  $\mu$ g/ml), muramyl dipeptide (MDP) (10  $\mu$ g/ml) for additional 6 hr. The conditioned media were collected for analyzing the level of caspase-1, IL-1 $\beta$ , IL-18 and TNF- $\alpha$  by immunoblotting or ELISA. The cell lysates were also harvested for analyzing the levels of pro-caspase-1, pro-IL-1 $\beta$  by immunoblotting. For analyzing the maturation of IL-1 $\beta$  and the activation of caspase-1, the conditioned media were collected and precipitated

by a chloroform-methanol method. 500  $\mu$ L of supernatant was mixed with 500  $\mu$ L of methanol and 125  $\mu$ L of chloroform (4:4:1). After vortex for 15 s, samples were centrifuged at 20,000  $\times$  g for 15 minutes and the upper phase of the mixture was discarded. 400  $\mu$ L of methanol were then added into the sample and centrifuged at 20,000  $\times$  g for 15 minutes. The supernatants were removed and the pellets were dried for 10 min. The pellets were resuspended in 2  $\times$  SDS loading buffer, boiled for 10 min at 95°C, and then subjected to immunoblot analysis.

For activation of the non-canonical inflammasome pathway, BMDMs were either not treated or primed with Pam3CSK4 for 3 h and further stimulated for 16 h with LPS that was transfected in a concentration of 1 mg/ml LPS in serum-free medium containing 0.25% (v/v) FuGENE HD (Promega). The conditioned media and cell lysate were collected and subjected for further analysis by western blotting and ELISA.

**LPS-induced endotoxin shock**—8-week-old of WT and Peli1 MKO mice were intraperitoneally injected with 25mg/kg (body weight) of LPS. The viability of these mice was monitored daily. The serum of mice was collected at 2 h after LPS injection for cytokine detection by ELISA.

**MCC950 treatment**—MCC950 was purchased from EMD Millipore (Catalog number: 538120). 8-week-old of WT and Peli1 MKO mice were intraperitoneally injected with 40 mg/kg (body weight) of MCC950 1 h before the injection of 25 mg/kg LPS. The viability of these mice was monitored daily. The serum of mice was collected at 2 h after LPS injection and then analyzed the level of IL-1 $\beta$  by ELISA.

**LDH activity assay**—WT and Peli1 KO BMDMs were treated with or without 1  $\mu$ g/ml LPS for 3.5 h and further stimulated with nigericin for 30 min. Supernatants were used to assay in triplicate using a Lactate Dehydrogenase (LDH) Activity Assay Kit (Cayman Chemical). The supernatants were mixed with 50  $\mu$ L Master Reaction Mix, and subjected for the detection of O.D. 450 using a microplate spectrophotometer (BioTek).

**Immunoblot, CoIP and ubiquitination assays**—BMDMs, iBMDMs and 293T cells were lysed in RIPA buffer containing 50 mM Tris-HCl (pH 7.4), 150 mM NaCl, 1% NP-40, 0.5% sodium deoxycholate, 1 mM EDTA, 1 mM dithiothreitol, 1 mM sodium orthovanadate, 5 mM sodium Fluoride, 20 mM p-nitrophenyl phosphate, 1 mM phenylmethylsulfonyl fluoride, 1mg/ml pepstatin and 1 mg/ml aprotinin. The whole-cell lysates were subjected to immunoblot and CoIP assays. For immunoblot, the cell lysates were subjected to SDS-PAGE and then transferred to nitrocellulose membranes. The membranes were blocked with 5% skim milk in PBST; the specific proteins were recognized by primary antibodies and subsequently by secondary antibodies conjugated with Horseradish peroxidase (Jackson, PA) in 5% skim milk. After incubation with Enhanced Chemiluminescence substrates, the signals of target proteins were detected by X-ray film processor. For CoIP assays, cell lysates were mixed with specific primary antibodies and gently rotated for 1h at 4°C. Protein A/G agarose beads were then added to the mixture for isolating the complexes by rotation for 2 h, the protein-bead complexes were then washed

four times using RIPA buffer. The precipitated proteins were boiled in 2x Laemmli sample buffer for 10 minutes and subjected to SDS-PAGE and immunoblot analysis.

For ubiquitination assays, BMDMs or transiently transfected 293T cells were lysed in RIPA buffer supplemented with 4 mM N-ethylmaleimide. The cell lysates were immediately boiled for 5 min in the presence of 1% (vol/vol) SDS, diluted ten times with RIPA buffer, and subjected to immunoprecipitation using the indicated antibodies and protein A or protein G agarose beads. After 5 washes with RIPA buffer, the precipitated proteins were subjected to SDS-PAGE and immunoblot analysis using antibodies detecting total ubiquitin chains.

**Flow cytometry and intracellular cytokine staining**—The cells were incubated for 15 min on ice with blocking anti-CD16/CD32 Ab supplemented with 1% BSA. The cells were stained with fluorescence-conjugated antibodies for 30 min on ice and subjected to flow cytometry or cell sorting essentially using LSR II (BD Bioscience) and FACSJazz (BD Bioscience) flow cytometers, respectively. Flow cytometry data were analyzed using FlowJo software.

**ASC Oligomerization and ASC-Speck Formation**—WT and Peli1 KO BMDMs were treated with or without 1 µg/ml LPS for 3.5 h and further stimulated with nigericin for 30 min. The cells were rinsed in ice-cold PBS, then the cells were harvested and lysed in 500 µL of ice-cold lysis buffer (50 mM Tris-HCl, pH 7.6, 0.5% Triton X-100, 0.1 mM PMSF and a protease inhibitor cocktail). Lysates were centrifuged at 330 X g for 10 min at 4°C. The pellets were washed twice with ice-cold PBS and resuspended in 500 µL PBS. 2 mM disuccinimidyl suberate (DSS) was added to the resuspended pellets, which were incubated at room temperature for 30 min with rotation. Samples were then centrifuged. The supernatant was removed, and the cross-linked pellets were resuspended in 30 mL of SDS loading buffer. Samples were boiled for 10 min at 95°C and analyzed by immunoblot analysis.

WT and Peli1 KO BMDMs were seeded to coverslips and treated with or without 1 mg/ml LPS for 3.5 h and further stimulated with nigericin for 30 min. Cells were fixed for 10 min with methanol and washed three times with PBS. The analysis of ASC speck was determined by using immunofluorescence staining of ASC using anti-ASC antibody and anti-rabbit Alexa Fluor 488. The cells were counter stained with DAPI. The summary result was calculated from the percentage of cells with positive ASC speck signal.

## QUANTIFICATION AND STATISTICAL ANALYSIS

Statistical analyses were performed using Prism (GraphPad v.8.0.0). For survival analysis, the survival rate was analyzed using the Kaplan–Meier method with differences determined by log-rank test. All other statistical analyses were performed by a two-tailed unpaired t test. P values of less than 0.05 were considered significant in all studies with the level of significance being denoted as \* $p < 0.05$ ; \*\* $p < 0.01$ ; \*\*\* $p < 0.001$ . Each experiment was repeated independently with similar results, and the number of independent experiments and number of animals in each experiment are indicated in figure legends.

## Supplementary Material

Refer to Web version on PubMed Central for supplementary material.

## ACKNOWLEDGMENTS

We thank the Knockout Mouse Project (KOMP) and the European Conditional Mouse Mutagenesis Program (EUCOMM) for the Peli1-targeted mice and BEI Resources for iBMDMs. This work was supported by grants from the National Institutes of Health (AI104519 and AI057555). This study also used the NIH/NCI-supported resources under award number P30CA016672 at The MD Anderson Cancer Center. T.G. was a visiting student supported by a scholarship from the China Scholarship Council (grant 201906380080).

## REFERENCES

- Broz P, and Dixit VM (2016). Inflammasomes: mechanism of assembly, regulation and signalling. *Nat. Rev. Immunol* 16, 407–420. [PubMed: 27291964]
- Broz P, von Moltke J, Jones JW, Vance RE, and Monack DM (2010). Differential requirement for Caspase-1 autoproteolysis in pathogen-induced cell death and cytokine processing. *Cell Host Microbe* 8, 471–483. [PubMed: 21147462]
- Chang M, Jin W, and Sun SC (2009). Peli1 facilitates TRIF-dependent Toll-like receptor signaling and proinflammatory cytokine production. *Nat. Immunol* 10, 1089–1095. [PubMed: 19734906]
- Coll RC, Robertson AA, Chae JJ, Higgins SC, Muñoz-Planillo R, Inserra MC, Vetter I, Dungan LS, Monks BG, Stutz A, et al. (2015). A small-molecule inhibitor of the NLRP3 inflammasome for the treatment of inflammatory diseases. *Nat. Med* 21, 248–255. [PubMed: 25686105]
- Eisenbarth SC, Colegio OR, O'Connor W, Sutterwala FS, and Flavell RA (2008). Crucial role for the Nalp3 inflammasome in the immunostimulatory properties of aluminium adjuvants. *Nature* 453, 1122–1126. [PubMed: 18496530]
- Fernandes-Alnemri T, Wu J, Yu JW, Datta P, Miller B, Jankowski W, Rosenberg S, Zhang J, and Alnemri ES (2007). The pyroptosome: a supramolecular assembly of ASC dimers mediating inflammatory cell death via caspase-1 activation. *Cell Death Differ* 14, 1590–1604. [PubMed: 17599095]
- Guan K, Wei C, Zheng Z, Song T, Wu F, Zhang Y, Cao Y, Ma S, Chen W, Xu Q, et al. (2015). MAVS Promotes Inflammasome Activation by Targeting ASC for K63-Linked Ubiquitination via the E3 Ligase TRAF3. *J. Immunol* 194, 4880–4890. [PubMed: 25847972]
- Guarda G, Braun M, Staehli F, Tardivel A, Mattmann C, Förster I, Farlik M, Decker T, Du Pasquier RA, Romero P, and Tschopp J (2011). Type I interferon inhibits interleukin-1 production and inflammasome activation. *Immunity* 34, 213–223. [PubMed: 21349431]
- Guo H, Callaway JB, and Ting JP (2015). Inflammasomes: mechanism of action, role in disease, and therapeutics. *Nat. Med* 21, 677–687. [PubMed: 26121197]
- He Y, Hara H, and Núñez G (2016). Mechanism and Regulation of NLRP3 Inflammasome Activation. *Trends Biochem. Sci* 41, 1012–1021. [PubMed: 27669650]
- Hu H, and Sun SC (2016). Ubiquitin signaling in immune responses. *Cell Res* 26, 457–483. [PubMed: 27012466]
- Humphries F, Bergin R, Jackson R, Delagic N, Wang B, Yang S, Dubois AV, Ingram RJ, and Moynagh PN (2018). The E3 ubiquitin ligase Pellino2 mediates priming of the NLRP3 inflammasome. *Nat. Commun* 9, 1560. [PubMed: 29674674]
- Jin W, Chang M, and Sun SC (2012). Peli: a family of signal-responsive E3 ubiquitin ligases mediating TLR signaling and T-cell tolerance. *Cell. Mol. Immunol* 9, 113–122. [PubMed: 22307041]
- Kayagaki N, Warming S, Lamkanfi M, Vande Walle L, Louie S, Dong J, Newton K, Qu Y, Liu J, Heldens S, et al. (2011). Non-canonical inflammasome activation targets caspase-11. *Nature* 479, 117–121. [PubMed: 22002608]
- Ko CJ, Zhang L, Jie Z, Zhu L, Zhou X, Xie X, Gao T, Yang JY, Cheng X, and Sun SC (2021). The E3 ubiquitin ligase Peli1 regulates the metabolic actions of mTORC1 to suppress antitumor T cell responses. *EMBO J* 40, e104532. [PubMed: 33215753]



- Lu A, Magupalli VG, Ruan J, Yin Q, Atianand MK, Vos MR, Schröder GF, Fitzgerald KA, Wu H, and Egelman EH (2014). Unified polymerization mechanism for the assembly of ASC-dependent inflammasomes. *Cell* 156, 1193–1206. [PubMed: 24630722]
- Magupalli VG, Negro R, Tian Y, Hauenstein AV, Di Caprio G, Skillern W, Deng Q, Orning P, Alam HB, Maliga Z, et al. (2020). HDAC6 mediates an aggresome-like mechanism for NLRP3 and pyrin inflammasome activation. *Science* 369, eaas8995. [PubMed: 32943500]
- Moynagh PN (2009). The Pellino family: IRAK E3 ligases with emerging roles in innate immune signalling. *Trends Immunol* 30, 33–42. [PubMed: 19022706]
- Moynagh PN (2014). The roles of Pellino E3 ubiquitin ligases in immunity. *Nat. Rev. Immunol* 14, 122–131. [PubMed: 24445667]
- Pasparakis M, Alexopoulou L, Episkopou V, and Kollias G (1996). Immune and inflammatory responses in TNF alpha-deficient mice: a critical requirement for TNF alpha in the formation of primary B cell follicles, follicular dendritic cell networks and germinal centers, and in the maturation of the humoral immune response. *J. Exp. Med* 184, 1397–1411. [PubMed: 8879212]
- Pfeffer K, Matsuyama T, Kündig TM, Wakeham A, Kishihara K, Shahinian A, Wiegmann K, Ohashi PS, Krönke M, and Mak TW (1993). Mice deficient for the 55 kd tumor necrosis factor receptor are resistant to endotoxic shock, yet succumb to *L. monocytogenes* infection. *Cell* 73, 457–467. [PubMed: 8387893]
- Rayamajhi M, Zhang Y, and Miao EA (2013). Detection of pyroptosis by measuring released lactate dehydrogenase activity. *Methods Mol. Biol* 1040, 85–90.
- Schroder K, and Tschopp J (2010). The inflammasomes. *Cell* 140, 821–832. [PubMed: 20303873]
- Shi H, Wang Y, Li X, Zhan X, Tang M, Fina M, Su L, Pratt D, Bu CH, Hildebrand S, et al. (2016). NLRP3 activation and mitosis are mutually exclusive events coordinated by NEK7, a new inflammasome component. *Nat. Immunol* 17, 250–258. [PubMed: 26642356]
- Sokolovska A, Hem SL, and HogenEsch H (2007). Activation of dendritic cells and induction of CD4(+) T cell differentiation by aluminum-containing adjuvants. *Vaccine* 25, 4575–4585. [PubMed: 17485153]
- Swanson KV, Deng M, and Ting JP (2019). The NLRP3 inflammasome: molecular activation and regulation to therapeutics. *Nat. Rev. Immunol* 19, 477–489. [PubMed: 31036962]
- Testa G, Schaft J, van der Hoeven F, Glaser S, Anastassiadis K, Zhang Y, Hermann T, Stremmel W, and Stewart AF (2004). A reliable lacZ expression reporter cassette for multipurpose, knockout-first alleles. *Genesis* 38, 151–158. [PubMed: 15048813]
- Vajjhala PR, Mirams RE, and Hill JM (2012). Multiple binding sites on the pyrin domain of ASC protein allow self-association and interaction with NLRP3 protein. *J. Biol. Chem* 287, 41732–41743. [PubMed: 23066025]
- Vanden Berghe T, Demon D, Bogaert P, Vandendriessche B, Goethals A, Depuydt B, Vuylsteke M, Roelandt R, Van Wouterghem E, Vandenbroecke J, et al. (2014). Simultaneous targeting of IL-1 and IL-18 is required for protection against inflammatory and septic shock. *Am. J. Respir. Crit. Care Med* 189, 282–291. [PubMed: 24456467]
- Xue Y, Enosi Tuipulotu D, Tan WH, Kay C, and Man SM (2019). Emerging Activators and Regulators of Inflammasomes and Pyroptosis. *Trends Immunol* 40, 1035–1052. [PubMed: 31662274]
- Yang Y, Wang H, Kouadir M, Song H, and Shi F (2019). Recent advances in the mechanisms of NLRP3 inflammasome activation and its inhibitors. *Cell Death Dis* 10, 128. [PubMed: 30755589]
- Zahid A, Li B, Kombe AJK, Jin T, and Tao J (2019). Pharmacological Inhibitors of the NLRP3 Inflammasome. *Front. Immunol* 10, 2538. [PubMed: 31749805]

**Highlights**

- Peli1 deficiency impairs NLRP3 inflammasome activation
- Peli1 deficiency ameliorates inflammasome-mediated inflammation in mice
- Peli1 conjugates K63 ubiquitin chains to ASC
- Peli1-mediated ASC ubiquitination facilitates ASC oligomerization

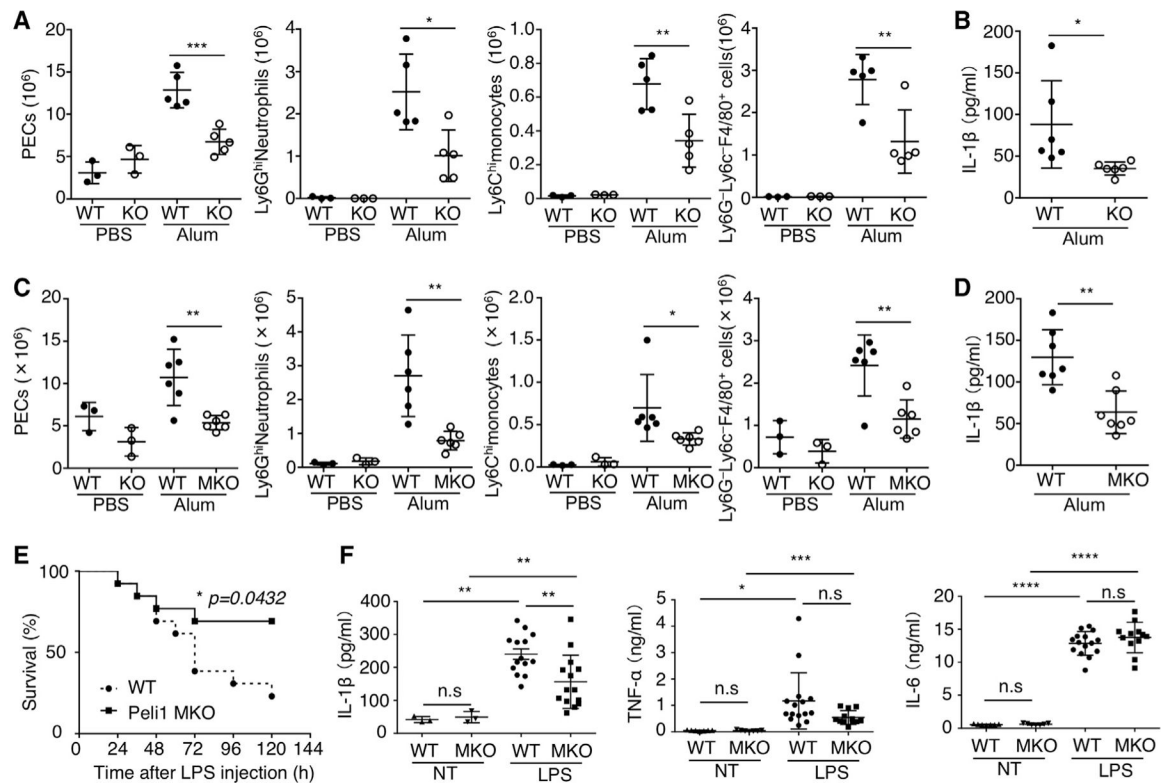


**Figure 1. Peli1 deficiency alleviates inflammation and reduces serum IL-1β**

(A) Peli1-WT (*Peli1*<sup>+/+</sup>) or KO (*Peli1*<sup>-/-</sup>) mice were injected intraperitoneally (i.p.) with PBS or aluminum salts (alum). After 14 h, PECs were counted, and neutrophils, monocytes, and mature macrophages were stained and analyzed by flow cytometry (PBS: WT, n = 3; KO, n = 3; alum: WT, n = 5; KO, n = 5).

(B) ELISA of IL-1β in peritoneal lavage fluid from Peli1-WT or KO mice 6 h after intraperitoneal injection of PBS or alum (WT, n = 6; KO, n = 6).

(C) Peli1-WT (*Peli1*<sup>+/+</sup>Lyz2-Cre) or MKO (*Peli1*<sup>fl/fl</sup>Lyz2-Cre; MKO) mice were injected i.p. with PBS or alum. After 14 h, PECs were counted, and neutrophils, monocytes, and mature macrophages were stained and analyzed by flow cytometry (PBS: WT, n = 3; KO, n = 3; alum: WT, n = 6; KO, n = 6).

(D) ELISA of IL-1β in peritoneal lavage fluid from Peli1-WT or MKO mice 6 h after intraperitoneal injection of PBS or alum (WT, n = 7; KO, n = 7).

(E and F) Survival curve (E) (WT, n = 13; KO, n = 13) and serum cytokine ELISA (F) (for IL-1β, not treated [NT]: WT, n = 3; KO, n = 3. LPS: WT, n = 14; KO, n = 14; for TNF-α and IL-6, NT: WT, n = 7; KO, n = 7; LPS: WT, n = 15; KO, n = 12) of Peli1-MKO or WT control mice i.p. injected with LPS (25 mg/kg body weight) for the indicated time points (E) or 2 h (F).

Data are representative of three independent experiments, and bar graphs are presented as mean ± SEM. p values were determined by a two-tailed unpaired Student's t test (A–D and F) or Kaplan-Meier method with a log-rank test (E): \*p < 0.05; \*\*p < 0.01; \*\*\*p < 0.001.

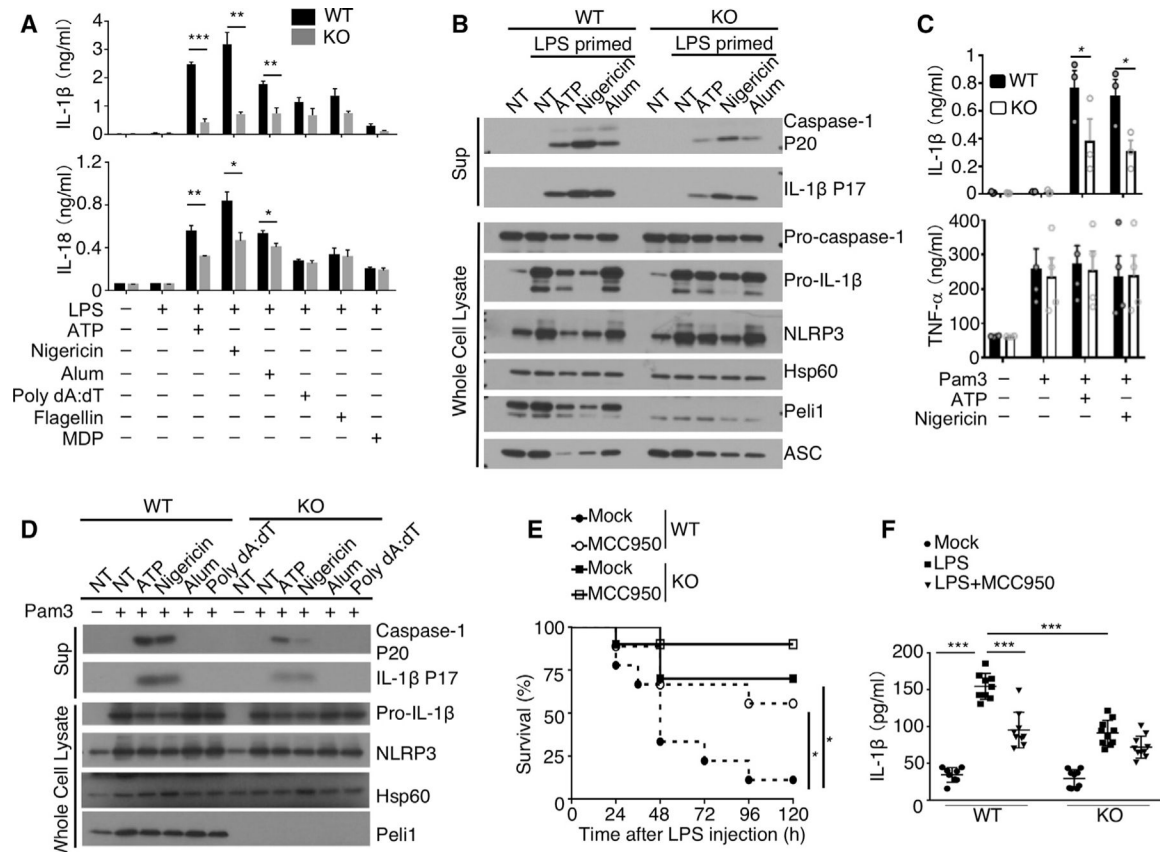


**Figure 2. Peli1 mediates activation of the NLRP3 inflammasome**

(A) WT and Peli1-KO BMDMs were treated with 1  $\mu$ g/mL LPS for 3.5 h with (+) or without (-) further stimulation with ATP, nigericin, alum, poly(dA:dT), flagellin, and MDP. The conditioned media were collected and subjected to ELISA to determine the level of IL-1 $\beta$  and IL-18 (WT, n = 3; KO, n = 3).

(B) WT and Peli1-KO BMDMs were either NT or primed with 1  $\mu$ g/mL LPS for 3.5 h followed by a further incubation without (NT) or with the indicated NLRP3 inducers. Cell lysates and precipitated conditioned media (Sup) were analyzed by immunoblotting to detect the indicated proteins.

(C) WT and Peli1-KO BMDMs were NT (-) or primed with 500 ng/mL Pam3CSK4 for 3.5 h with (+) or without (-) further stimulation with ATP and nigericin for 30 min. Conditioned media were collected for ELISA to determine the level of IL-1 $\beta$  and TNF- $\alpha$  (for IL-1 $\beta$ : WT, n = 3; KO, n = 3; for TNF- $\alpha$ : WT, n = 4; KO, n = 4).

(D) WT and Peli1 KO BMDMs were primed with (+) 500 ng/mL Pam3CSK4 for 3.5 h and then further incubated without (NT) or with the indicated inflammasome inducers. Cell lysates and precipitated conditioned media (Sup) were analyzed by immunoblotting to detect the indicated proteins.

(E and F) 8-week-old Peli1-KO or WT control mice were i.p. injected with MCC950 for 2 h before LPS challenge. The serum was collected 2 h later for IL-1 $\beta$  ELISA, and mouse viability was monitored daily (WT, n = 9; KO, n = 10).

Data are representative of three independent experiments, and bar graphs are presented as mean  $\pm$  SEM of biological replicates. p values were determined by a two-tailed unpaired Student's t test (A, C and F) or Kaplan-Meier method with a log-rank test (E): \*p < 0.05; \*\*p < 0.01; \*\*\*p < 0.001.

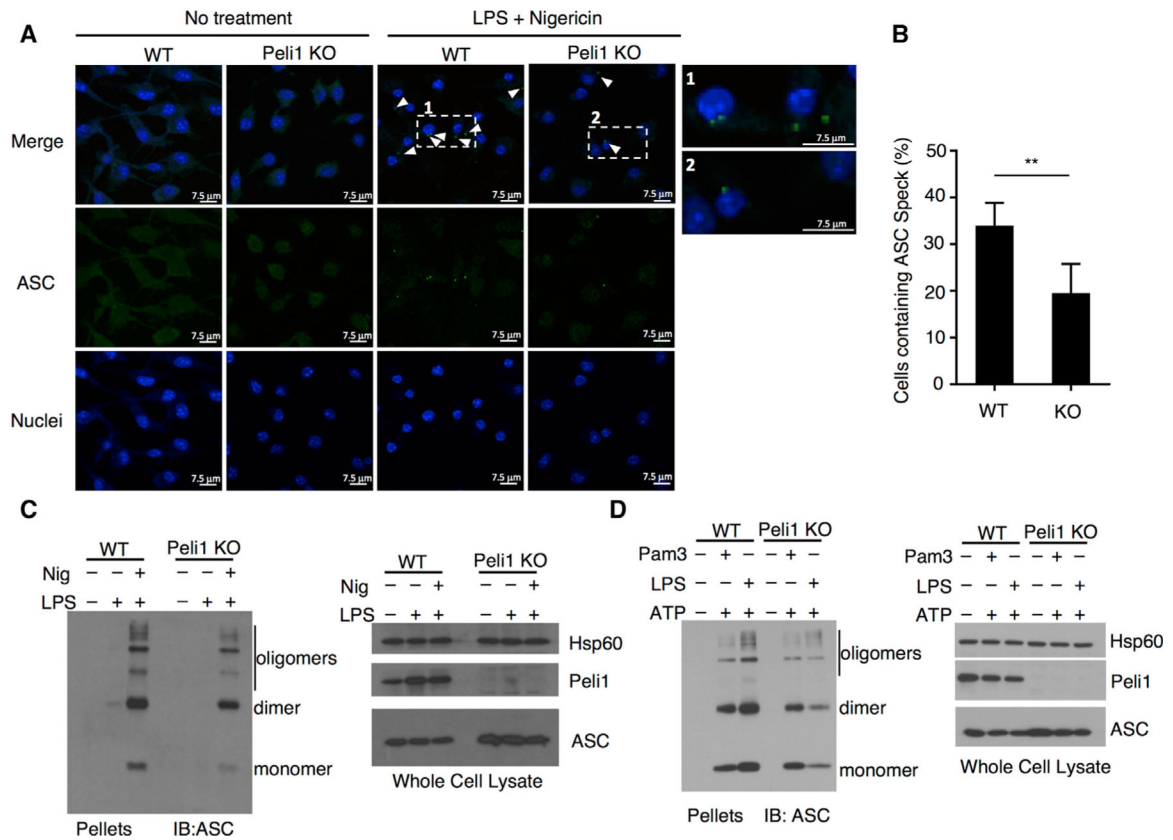


**Figure 3. Peli1 mediates ASC oligomerization and speck formation**

(A and B) WT and Peli1 KO BMDMs were either NT or primed with 1  $\mu$ g/mL LPS for 3.5 h and further stimulated with nigericin for 30 min. ASC specks were detected by immunofluorescence staining using anti-ASC (green) and counterstaining using DAPI (blue). Scale bar, 7.5  $\mu$ m. (A). Quantified data are presented as mean  $\pm$  SEM of the percentage of cells with ASC speck formation based on biological replicates (B) (WT, n = 5; KO, n = 5). p values were determined by a two-tailed unpaired Student's t test: \*\*p < 0.01.

(C) Analysis of ASC oligomerization in WT and Peli1-KO BMDMs primed with 1 mg/mL LPS for 3.5 h and further stimulated with (+) or without (–) nigericin for 30 min. Cells were cross-linked by DSS reagent, and the insoluble cross-linked fraction was subjected to immunoblot with anti-ASC (left). An immunoblot using whole-cell lysates were included to show protein expression levels (right).

(D) Analysis of ASC oligomerization in WT and Peli1-KO BMDMs primed with 1  $\mu$ g/mL LPS or 500 ng/mL Pam<sub>3</sub>CSK<sub>4</sub> for 3.5 h and further stimulated with (+) or without (–) ATP for 15 min. Immunoblots were performed using insoluble cross-linked fraction and anti-ASC (left) or whole-cell lysates for detecting the indicated proteins (right). Data are representative of three independent experiments



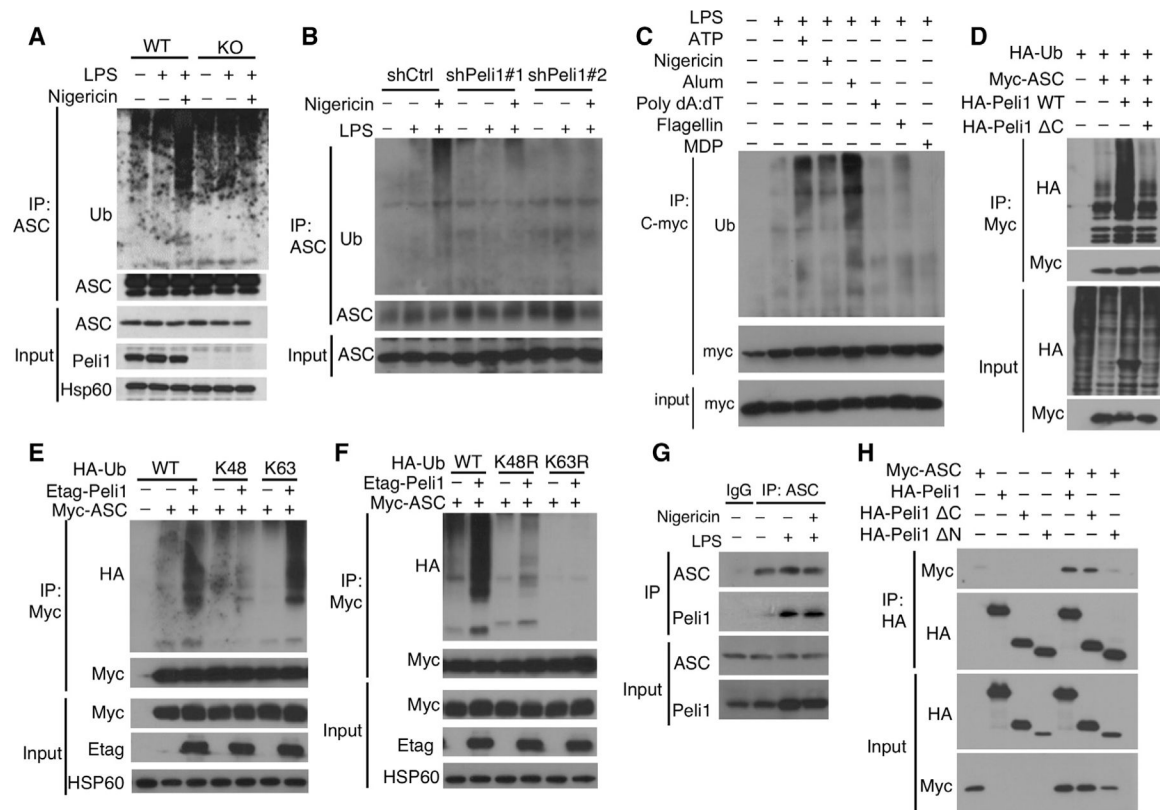


**Figure 4. Peli1 interacts with ASC and mediates ASC ubiquitination**

(A) Immunoblot analysis using anti-ubiquitin to detect ubiquitination of endogenous ASC following its immunoprecipitation from WT or Peli1-KO BMDMs treated as indicated (upper). Cell lysates (input) were also subjected to immunoblot to detect expression of the indicated proteins (lower).

(B) Ubiquitination analysis of endogenous ASC immunoprecipitated from Peli1 knockdown (using two different shRNA) or control iBMDMs, primed with LPS and further stimulated with nigericin for 45 min.

(C) Ubiquitination analysis of exogenous ASC immunoprecipitated from Myc-ASC-transduced iBMDMs primed with LPS for 3 h and further stimulated for 45 min with nigericin and ATP or stimulated for 6 h with alum, poly dA:dT, flagellin, and MDP.

(D–F) Ubiquitination analysis of exogenous ASC immunoprecipitated from 293T cells transfected with WT hemagglutinin (HA)-tagged ubiquitin (D) or WT and mutant forms of HA-ubiquitin (E and F) along with (+) the indicated expression vectors.

(G) CoIP analysis of endogenous Peli1-ASC interaction in BMDMs primed with LPS (1 μg/mL) for 3.5 h with (+) or without (–) further stimulation for 30 min with nigericin. ASC complex was isolated by immunoprecipitation, and the precipitated ASC and Peli1 proteins were detected by immunoblot using anti-Peli1 and anti-ASC.

(H) CoIP analysis of exogenous ASC and Peli1 or Peli1 mutants in transfected HEK293 cells transiently transfected with the indicated expression vectors. Data are representative of three independent experiments.

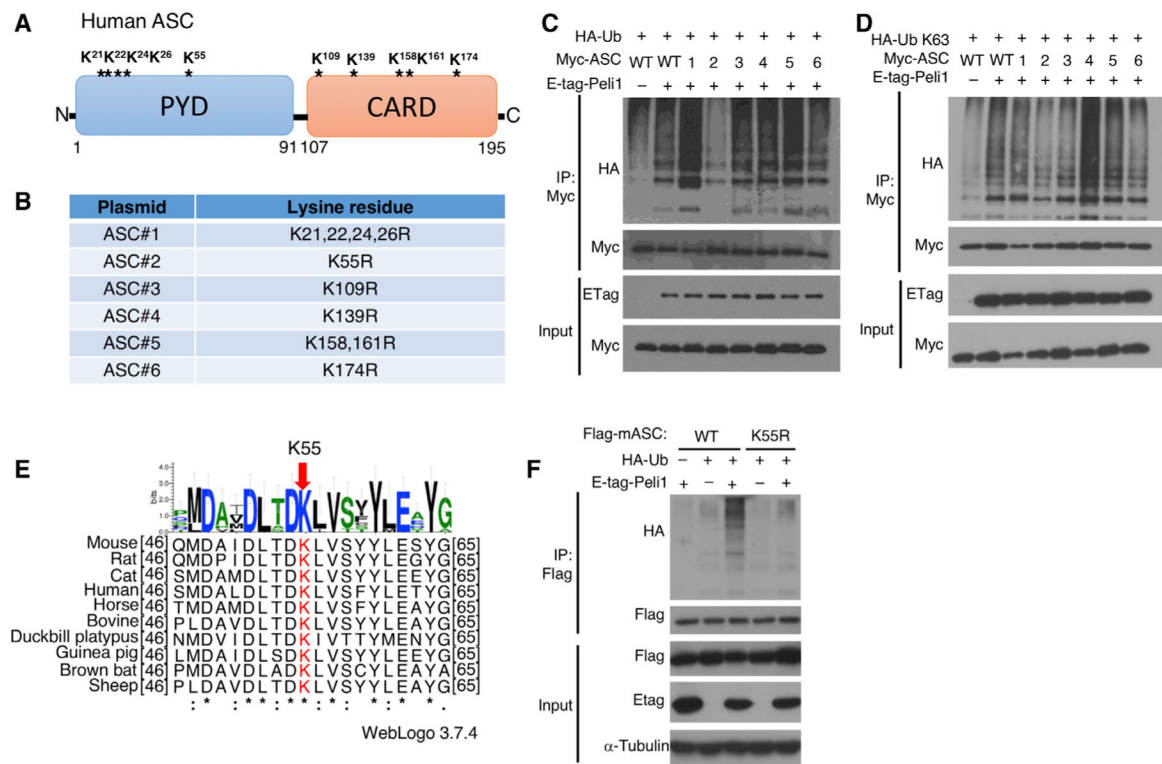


**Figure 5. K55 of ASC is required for its ubiquitination by Peli1**  
(A) A diagram of human ASC with its lysine (K) residues and domains indicated.  
(B) A list of the six human ASC mutants harboring the indicated lysine-to-arginine substitutions.  
(C and D) 293T cells were transiently transfected with Myc-tagged human WT ASC or the six ASC mutants listed in (B), along with the indicated expression vectors. ASC and mutants were isolated by immunoprecipitation using anti-Myc and subjected to immunoblot with anti-HA to detect ASC ubiquitination.  
(E) Amino acid sequence alignment of ASC from different species, highlighting the conserved lysine residue K55.  
(F) Analysis of ubiquitin conjugation to mouse ASC WT and K55R mutant expressed in 293T cells along with (+) or without (-) HA-ubiquitin and E-tag-Peli1. Data are representative of three independent experiments.

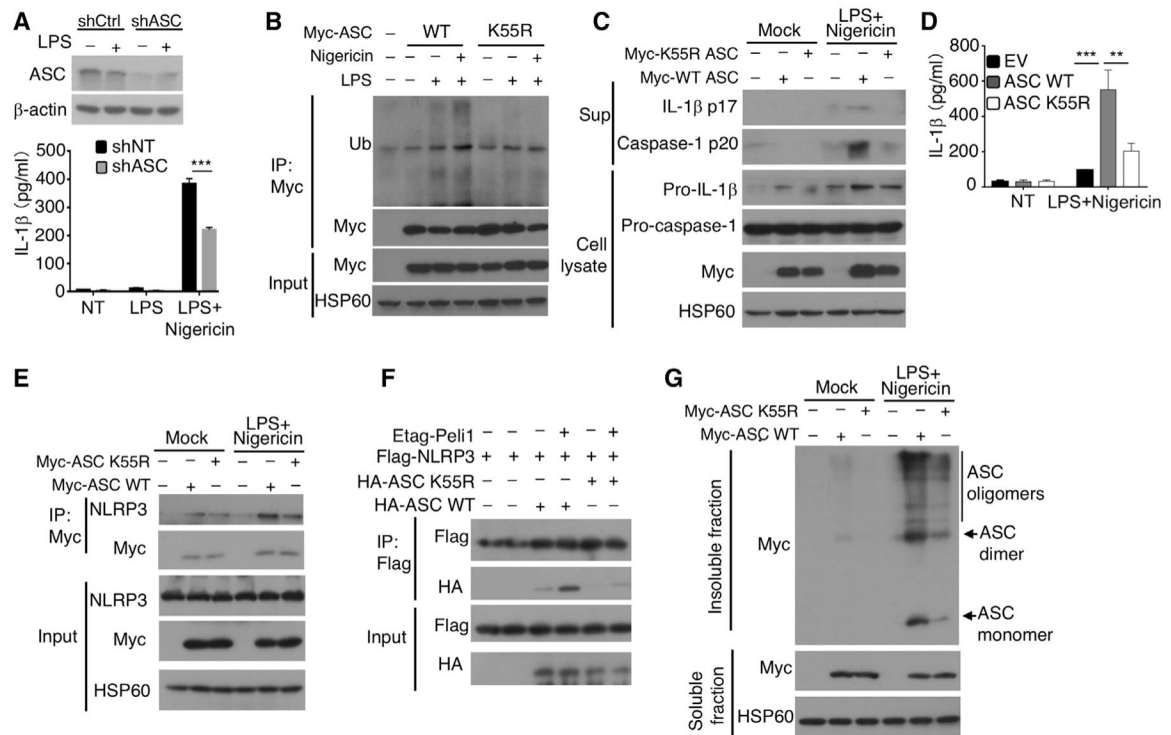


**Figure 6. K55 ubiquitination of ASC is critical for NLRP3 inflammasome activation**

(A) Immunoblot analysis of ASC in whole-cell lysates (upper) and ELISA of IL-1β in conditioned media (lower) of control and ASC-knockdown iBMDMs treated as indicated (WT, n = 4; KO, n = 4).

(B) Immunoblot analysis to detect ubiquitination of ASC immunoprecipitated from lysates of ASC-knockdown iBMDMs stably transduced with (+) ASC WT or K55R and primed with LPS for 3 h with further stimulation for 1 h with nigericin.

(C and D) ASC-knockdown iBMDMs reconstituted (by retroviral infection) with (+) or without (–) ASC WT or K55R were primed with LPS for 3 h and further stimulated for 1 h with nigericin. Inflammasome activation was determined by immunoblotting analysis of precipitated conditional media (Sup) or cell lysates (C) or ELISA analysis of IL-1β in conditioned media (D) (WT, n = 3; KO, n = 3).

(E) CoIP analysis to determine the interaction of endogenous NLRP3 with ASC or ASC K55R using ASC-knockdown iBMDMs rescued with (+) or without (–) ASC WT or K55R. The cells were primed with LPS for 3 h and further stimulated for 1 h with nigericin.

(F) CoIP assays to determine Peli1-stimulated interaction between transfected NLRP3 and ASC or ASC K55R in 293T cells.

(G) ASC-knockdown iBMDMs rescued with (+) or without (–) ASC WT or K55R were primed with LPS for 3 h and further stimulated for 1 h with nigericin. ASC oligomerization was detected by anti-Myc immunoblot using insoluble cross-linked fraction (upper), and ASC expression was analyzed using soluble fraction. Data are representative of three independent experiments, and bar graphs are presented as mean ± SEM. p values were determined by a two-tailed unpaired Student's t test (A and D): \*\*p < 0.01; \*\*\*p < 0.001.

## KEY RESOURCES TABLE

Antibody, Reagent or Resource	Source	Identifier
<b>Antibodies</b>		
Anti-ubiquitin	Santa Cruz	Cat# sc-8017; RRID:AB_2762364
Anti-Peli1	Santa Cruz	Cat# sc-271065; RRID:AB_10610358
Anti-actin	Sigma-Aldrich	Cat# A2228; RRID:AB_476697
Horseradish-peroxidase-conjugated anti-Flag	Sigma-Aldrich	Cat# A8592; RRID:AB_439702
Myc-Tag	Cell Signaling Technology	Cat# 2278; RRID:AB_490778
Horseradish-peroxidase-conjugated anti-HA	Sigma-Aldrich	Cat# H6533; RRID:AB_439705
Horseradish-peroxidase-conjugated anti-Etag	Thermo Fisher Scientific	Cat# PA1-21895; RRID:AB_558708
Anti-IL-1 $\beta$	R&D	Cat# AF-401-NA; RRID:AB_416684
Anti-NLRP3	AdipoGen	Cat# AG-20B-0014; RRID:AB_2490202
anti-Caspase-1	AdipoGen	Cat# AG-20B-0042; RRID:AB_2490248
Anti-ASC	AdipoGen	Cat# AG-25B-0006; RRID:AB_2490440
Anti-mouse CD11b-eFluor 450	Thermo Fisher Scientific	Cat# 48-0112-82; RRID:AB_1582236
anti-mouse F4/80-PerCP-Cyanine5.5	Thermo Fisher Scientific	Cat# 45-4801-82; RRID:AB_914345
anti-mouse Ly6G-APC	Thermo Fisher Scientific	Cat# 17-9668-82; RRID:AB_2573307
anti-mouse Ly6C-PE-Cyanine7	Thermo Fisher Scientific	Cat# 25-5932-82; RRID:AB_2573503
Anti-CD16/CD32	Thermo Fisher Scientific	Ca# 14-0161-85; RRID:AB_467134
<b>Reagents</b>		
Nigericin	Invivogen	Catalog# tlrl-nig
Flagellin	Invivogen	Catalog# tlrl-stfla
Muramyl dipeptide	Invivogen	Catalog# tlrl-lmdp
poly(dA:dT)	Sigma-Aldrich	Catalog# P0883
Alum	Thermo Fisher Scientific	Catalog# 77161
Disuccinimidyl suberate	Thermo Fisher Scientific	Catalog# 21655
LPS	Sigma-Aldrich	Catalog# L2630
Pam3CSK4	Invivogen	Catalog# tlrl-pms
MCC950	EMD Millipore	Catalog# 538120
Val-boroPro	MedChemExpress	Catalog# HY-13233A
FuGENE <sup>®</sup> HD Transfection Reagent	Promega	Catalog# E2311
DAPI Staining Solution	Abcm	Catalog# ab228549
Dehydrogenase (LDH) Activity Assay Kit	Cayman Chemical	Catalog# 601171
<b>Plasmid</b>		
HA-tagged Peli1	Gift from S.H. Park (Sungkyunkwan University)	N/A
Etag-Peli1	Gift from R. Beyaert (Ghent University)	N/A
pcDNA3-HA-NEK7	Nat Immunol. 2016 Mar;17(3):250-8. <a href="https://doi.org/10.1038/ni.3333">https://doi.org/10.1038/ni.3333</a>	Bruce Beutler (Addgene plasmid # 75142)
pcDNA3-Flag-NLRP3	Nat Immunol. 2016 Mar;17(3):250-8. <a href="https://doi.org/10.1038/ni.3333">https://doi.org/10.1038/ni.3333</a>	Bruce Beutler (Addgene plasmid # 75127)
pcDNA3-Myc-ASC	Bryan et al. J Immunol. 2009 Mar 1;182(5):3173-82. doi:10.4049/jimmunol.0802367.	Christian Stehlik (Addgene plasmid # 73952)

Antibody, Reagent or Resource	Source	Identifier
pcDNA3-Flag-ASC	Nat Immunol. 2016 Mar;17(3):250-8. <a href="https://doi.org/10.1038/ni.3333">https://doi.org/10.1038/ni.3333</a>	Bruce Beutler (Addgene plasmid # 75134)
pcDNA3-Flag-Caspase-1	Nat Immunol. 2016 Mar;17(3):250-8. <a href="https://doi.org/10.1038/ni.3333">https://doi.org/10.1038/ni.3333</a>	Bruce Beutler (Addgene plasmid # 75128)
pRK5-HA-Ubiquitin-WT	Lim et al. J Neurosci. 2005 Feb 23. 25(8):2002-9.	Ted Dawson (Addgene plasmid # 17608)
pRK5-HA-Ubiquitin-K48	Lim et al. J Neurosci. 2005 Feb 23. 25(8):2002-9.	Ted Dawson (Addgene plasmid # 17605)
pRK5-HA-Ubiquitin-K63	Lim et al. J Neurosci. 2005 Feb 23. 25(8):2002-9.	Ted Dawson (Addgene plasmid # 17606)
HA-tagged ubiquitin K48R	Gift from Z. Chen (University of Texas Southwestern Medical Center)	N/A
HA-tagged ubiquitin K63R	Gift from Z. Chen (University of Texas Southwestern Medical Center)	N/A
pMSCV-IRES-mCherry FP	a gift from Dario Vignali	Dario Vignali (Addgene plasmid # 52114)
pMSCV-IRES-mCherry ASC WT	This study	N/A
pMSCV-IRES-mCherry ASC K55R	This study	N/A
pCI-ASC-HA	Hornung et al. Nature. 2009 Mar 26. 458(7237):514-8.	Kate Fitzgerald (Addgene plasmid # 41553)
<b>Experimental models: mouse model</b>		
Peli1 <sup>tm1a(EUCOMM)Wtsi</sup>	KOMP Repository program, University of California, Davis	MGI:4433689
Peli1 <sup>tm1b(EUCOMM)Wtsi</sup>	KOMP Repository program, University of California, Davis	MGI:6346891
B6.129S4-Gt(ROSA)26Sor <sup>tm1(FLP1)Dym/RainJ</sup>	The Jackson Laboratory	Stock No: 009086
B6.129P2-Lyz2 <sup>tm1(cre)lfo/J</sup>	The Jackson Laboratory	Stock No: 004781
Peli1 <sup>fl/fl</sup> Lyz2-Cre	This study	N/A
<b>Experimental models: Cell line</b>		
293T	ATCC	Catalog# CRL-3216
Murine immortalized bone marrow-derived macrophage	BEI Resources	Catalog# NR-9456
<b>Software and algorithms</b>		
GraphPad v.8.0.0	GraphPad Software	<a href="https://www.graphpad.com/scientific-software/prism/">https://www.graphpad.com/scientific-software/prism/</a>
Flowjo	BD (Becton, Dickinson & Company)	<a href="https://www.flowjo.com/">https://www.flowjo.com/</a>
ImageJ	Rasband, W.S., ImageJ, U. S. National Institutes of Health, Bethesda, Maryland, USA	<a href="https://imagej.nih.gov/ij/download.html">https://imagej.nih.gov/ij/download.html</a>